Progress In Electromagnetics Research C, Vol. 71, 69–77, 2017

A Dual Band Slot Antenna for Wireless Applications with Circular Polarization

Azadeh Pirooj[1], Mohammad Naser-Moghadasi[1], Ferdows B. Zarrabi[2, *], and Alireza Sharifi[1]

Abstract—In recently developed wireless communication systems, circular polarization (CP) antennas are used for communication links to reduce the natural loss effect in receivers. Therefore, in this paper, a dual-band microstrip slot antenna based on a parallel split ring resonator with circular and linear polarization which can be used for wireless and WiMAX applications is presented. The final antenna to design is based on inspired split ring resonators (SRR) to achieve circular polarization and compact size and with special parallel form of the SRR and straight feed line. We have achieved higher bandwidth in the requested frequency range with dual-band characteristics. The final antenna has a bi-directional pattern with circular polarization at the range of 2.9–3.65 GHz and bandwidths of 2–3.6 and 3.8–4.8 GHz with VSWR < 2 for WLAN, Bluetooth and radar applications for IEEE WLAN protocol with gain of 5–6 dBi, respectively. The size of the prototype patch antenna is $40 \times 40\,\text{mm}^2$. It is designed and fabricated on an FR-4 low cost substrate with $\varepsilon_r = 4.4$ and a thickness of 1.6 mm. It is simulated using HFSS full wave software. In addition, the experimental results are presented and compared with simulation for VSWR, radiation patterns and axial ratio. The periodic analysis has been used for extracting the metamaterial parameters.

1. INTRODUCTION

During the last decade, much research has been done on the development of left-handed Metamaterials (LHMs) due to their special and unique properties such as negative permittivity and permeability that are not found in nature [1, 2]. Metamaterials are more frequently used in antenna and microwave circuits, in order to increase the bandwidth and miniaturize the antenna [3, 4]. Generally, metamaterials include DNG (double negative) and SNG (single negative). ENGs (epsilon negative) are a group of SNGs with negative ε [5].

Therefore, a split ring resonator (SRR) is introduced because of its left-hand (LH) characteristics, and it is made by two concentric metallic rings with gaps in each ring on opposite sides in rectangular and circular forms [6, 7].

However, recently various shapes of these metamaterials have been used for making a frequency notched in UWB antenna with circular and rectangular slots in the monopole antenna or feed line [8, 9], miniaturization of the waveguide for filter designing [10, 11] or microstrip band-pass filter (BPF) with a broad-side coupled triple split-ring resonator (T-SRR) [12], and SRR and Defected Ground Structure (DGS) are combined in one structure [13].

Split ring resonator (SRR) elements are known as a special parasitic form of metamaterials which are used in microstrip antenna and filter design [14–16] where the ring plays the role of a resonator with the gap working as a capacitance and metal strip ring as an inductance in our circuit [15]. In addition,

Received 14 November 2016, Accepted 5 January 2017, Scheduled 30 January 2017

* Corresponding author: Ferdows B. Zarrabi (ferdows.zarrabi@yahoo.com).

[1] Faculty of Engineering, Science and Research Branch, Islamic Azad University, Tehran, Iran. [2] Young Researchers and Elite Club, Babol Branch, Islamic Azad University, Babol, Iran.

the coupling between rings has developed some new inductance and capacitance and multi-resonance devices which are noticed in antenna and microwave multi-band applications [17], and in this paper, we notice this quality in the microstrip antenna.

In addition, two different models of implementations of SRR slot and load for circular polarization (CP) are studied by Zarrabi et al. [18, 19]. They show that metamaterial loading can make circular polarization by controlling the current distribution on the surface of patch or slot antenna.

Typically, circular polarizations in antennas reduce the losses caused by multipath effects, between the transmitter and receiver antennas. The CP antenna, because of its low profile, small size, and lightweight, is attractive for portable wireless application such as Tablets. Therefore, a circular slot antenna with TE_{11} mode and a c-strip metal for circular polarization is given in [20].

Various methods for achieving circular polarization in microstrip antennas are available, such as using triple proximity-fed method by adjusting 120° phase shift between the feeds [21], circular polarization synthetic aperture radar (CP-SAR) operated in L-band by using the elliptical slot [22]. In addition, truncation or corner stubs are the conventional methods for achieving UWB characteristics with circular polarization by coplanar waveguide feed (CPW) [23, 24]. However, there exist various methods for generating circular polarization in slot antennas such as square-ring slot antenna fed with an L-shaped coupling strip for Wi-Fi application at 2.5 GHz [25], dual-square-ring-shaped slot for WiMAX applications at 3 GHz [26], and two-slot rings for 1.6 and 2.5 GHz [27]. CPW feed slot antennas are noticed for their facility of achieving circular polarization by means of two asymmetrical C-shaped strips with dual-band characteristics at 2.5 and 5.2 GHz [28] and corner truncated ground [29].

In this paper, we use a slot antenna with straight taper feed for excitation and a novel parallel modified SRR shape for achieving dual-band characteristics and circular polarization. The antenna design procedure is discussed, and the effect of antenna elements on S_{11} is investigated. Next, the current distribution is studied and shows how SRR elements change the current distribution in the final antenna model. Axial ratio and radiation patterns are presented as evidence for circular polarization in the final antenna. The simulated results are compared with experimental ones. The final antenna covers 3.3–3.8 GHz used for WiMAX applications and 3.4–4.2 GHz used for IMT advanced system or fourth generation (4G) mobile communication systems.

2. ANTENNA STRUCTURE

Figures 1(a) and 1(b) show the final modeled antenna ground and feed geometry, respectively. The final antenna model contains a circular slot on the ground layer. A circular slot radius of 13.5 mm is assumed, and a special form of SRR (split ring resonator) with parallel rings is used for miniaturization and circular polarization. For modification of the bandwidth and circular polarization, two triangular section cuttings in the ground plane are made in the final antenna.

The microstrip line feed of the proposed antenna is connected to a 50 Ω SMA connector as shown in Fig. 1(b) with 2 mm width. The prototype antenna is simulated using HFSS for full-wave electromagnetic field simulation, and it is fabricated on an FR-4 low cost dielectric substrate with relative permittivity of 4.4, loss tangent of 0.02, thickness of 1.6 mm and total area of $40 \times 40\,mm^2$. Fig. 1(c) shows the fabricated antenna, and four steps of the process of designing the antenna are presented in Fig. 1(d). In addition, all dimensions are presented in Table 1.

3. METAMATERIAL MODELING

Metamaterials are known as artificial materials and can be designed using various shapes such as SRR structures where the gaps identify left-hand capacitances, and strips identify inductances. These metamaterial structures that have negative permittivity and negative permeability are known as double negative metamaterials. The metamaterials are used for various applications such as reducing the mutual coupling by controlling the electrical field and antenna surface current [30]. For calculating the permittivity and permeability, various techniques such as Nicolson-Rose as a method have been developed, and these methods are based on scattering parameters with calculations done via Matlab. For this purpose, the magnitude and phase of S_{11} and S_{21} for the unit cell are extracted using HFSS, and the permittivity and permeability are obtained by Matlab [31].

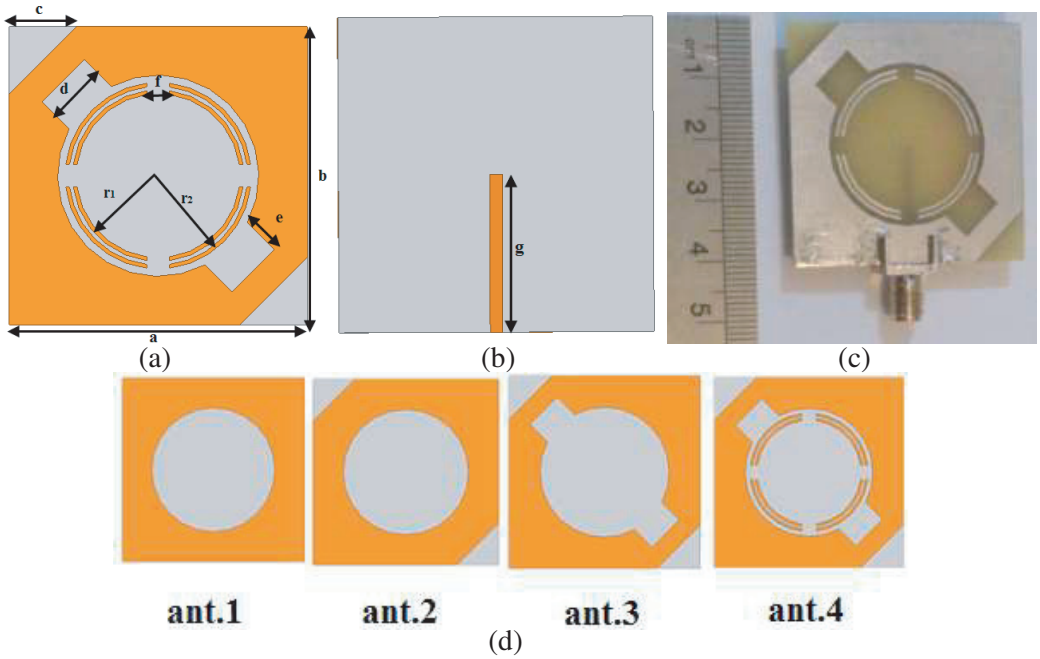

Figure 1. Geometrical model of the antenna. (a) Ground of antenna with the novel SRR, (b) corner feed line, (c) the prototype fabricated antenna, (d) four-steps of the process of designing the antenna.

Table 1. Geometrical parameters of the proposed antenna.

parameter	mm
a	4
b	4
c	9
d	8
e	6
f	3
g	20
r_1	11
r_2	12

Based on periodic boundary conditions and Floquet port or wave port for a three-dimensional unit cell, the S parameters are extracted, and by reflection and transmission, we can obtain S_{11} and S_{12} by Eqs. (1) and (2) where d is the thickness of the slab, k the wavenumber, n the refractive index and $R_{01} = \frac{Z-1}{Z+1}$ [31].

$$S_{11} = \frac{R_{01}\left(1 - e^{i2nk_0d}\right)}{1 - R_{01}^2 e^{i2nk_0d}} \tag{1}$$

$$S_{21} = \frac{\left(1 - R_{01}^2\right) e^{i2nk_0d}}{1 - R_{01}^2 e^{i2nk_0d}} \tag{2}$$

Using Equations (1) and (2), we can obtain Eq. (3) for impedance Z of the slab, and the refractive index is calculated by Eq. (4). The permittivity (ε) and permeability (μ) are related to the refractive

index and are obtained by $\varepsilon = n/Z$ and $\mu = nZ$, respectively [31].

$$Z = \pm\sqrt{\frac{(1+S_{11})^2 - S_{21}^2}{(1-S_{11})^2 - S_{21}^2}} \tag{3}$$

$$n = \frac{1}{k_0 d}\left[\left\{\left[\ln(e^{ink_0d})\right]'' + 2m\pi\right\} - i\left[\ln(e^{ink_0d})\right]'\right] \tag{4}$$

In Fig. 2, we have shown the permittivity and permeability for the proposed unit cell in the antenna. As shown here, the particles show negative real part of the permittivity and permeability for frequency bandwidth in the range of 3.2–4 GHz where the proposed antenna generates circular polarization at this frequency.

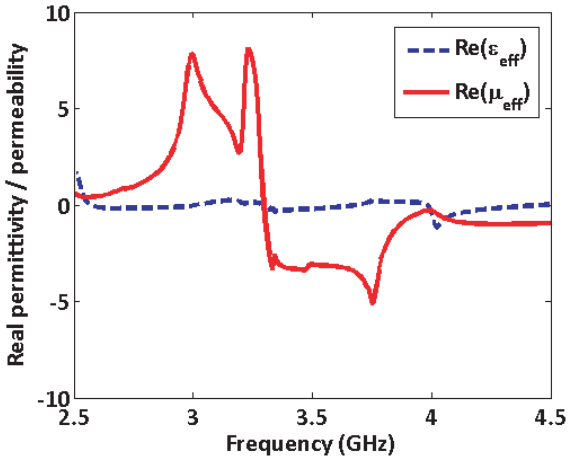

Figure 2. Real permittivity and permeability for the metamaterial unit cell.

4. SIMULATION AND EXPERIMENTAL RESULTS

Figure 3(a) shows the magnitude of S_{11} for antennas 1 to 4 in Fig. 1(d) in the range of 2–5 GHz. As shown here, the first antenna, (Ant. 1) has no any resonance in the range of 2–5 GHz when the two

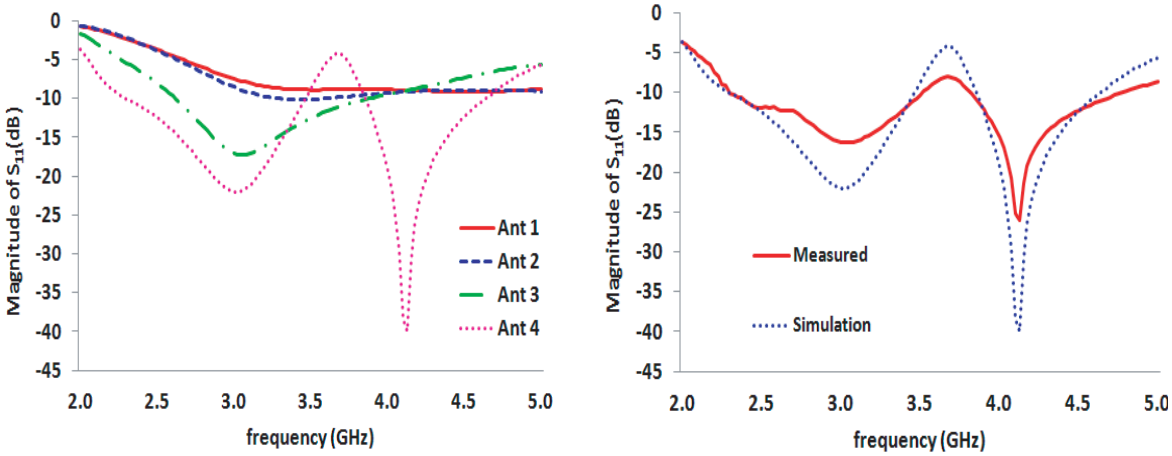

(a) (b)

Figure 3. Magnitude of S_{11} (a) for antennas 1 to 4, (b) for antenna 4, obtained using simulation and measurements.

triangular truncated slots are used in the ground, and the second antenna covers 3.3–3.6 GHz. So the truncated structure (Ant. 2) has larger bandwidth than the simple circular slot antenna. In the third step, by adding rectangular slots, the axial ratio of the antenna is improved; however, the magnitude of S_{11} is affected a little. In this case, the effective length is increased, and antenna impedance is matched with larger bandwidth (covering 2.6–3.9 GHz), so that it can cover the WiMAX and Bluetooth systems. Also, the first resonance is reduced, so that the antenna can be miniaturized. Fig. 3(a) shows that the final antenna (Ant. 4) operates as a dual-band antenna in 2.3–3.45 and 3.85–4.65 GHz for Wi-Fi, Bluetooth, WiMAX and LTE applications and that in this bandwidth, VSWR is less than 2 (magnitude of $S_{11} < -10$ dB) yielding 39% and 18% bandwidths respectively. Furthermore, comparison between the simulation and experiment results obtained using HFSS and HP8722ET network analyzer is presented in Fig. 2(b). The plots show that there is good matching between simulated and measured results.

Figure 4 shows simulations of the surface current vector distribution in HFSS for the final prototype antenna at 3.4 and 4.2 GHz for top and bottom faces in a 2D view. At the first frequency, the antenna's largest current occurs at the edge of rectangular slot as shown in Fig. 4(a). The truncated slot plays an important role by making a rotation in the current distribution, so that circular polarization is obtained at 3.4 GHz. Fig. 4(b) shows the antenna current distribution at 4.2 GHz, and at this frequency, the maximum value of the current is concentrated at the feed part with additive distribution. Therefore, the antenna has linear polarization. By comparison between current distribution (Fig. 4) and metamaterial

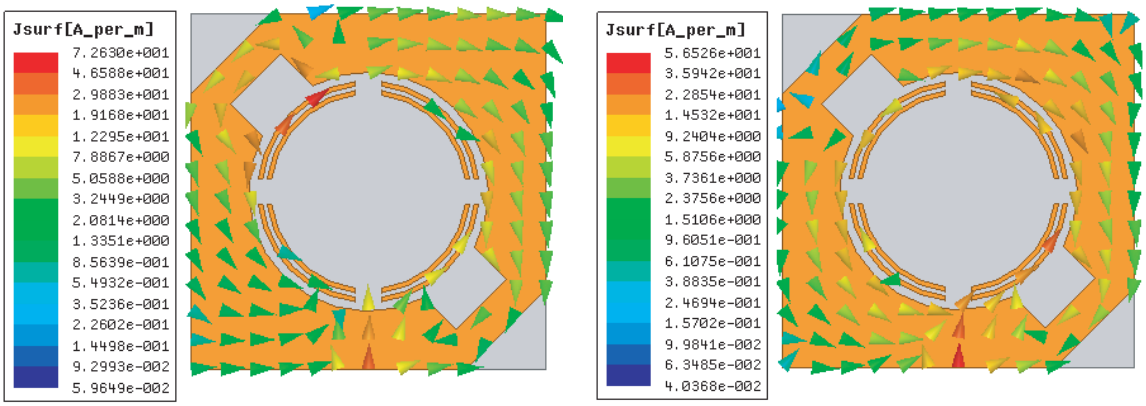

(a) (b)

Figure 4. The prototype antenna surface current distribution at (a) 3.4 GHz, (b) 4.2 GHz.

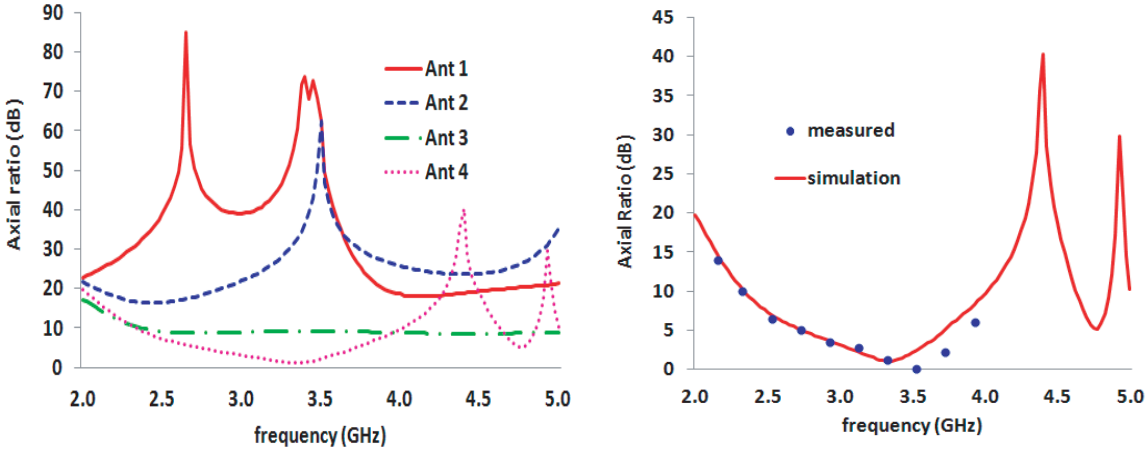

(a) (b)

Figure 5. Axial ratio (a) for the 4 steps of the design process, (b) for the final antenna, obtained using simulation and measurements.

characteristics in Fig. 2, we realize that at 3.4 GHz the negative value of the metamaterial part has caused a current distribution in opposite directions on the ring, and it has made circular polarization.

Figure 5(a) shows the axial ratio for antennas 1 to 4 in the range of 2–5 GHz. As shown here, axial ratio of the first antenna is more than 3 dB (over the 20 dB) in the range of 2–5 GH, and therefore, this antenna has linear polarization (Ant. 1). In the second model (Ant. 2), when the corner truncation is added to the slot antenna, the axial ratio is reduced in comparison to the first antenna, but in this case, the axial ratio is still more than 3 dB (over the 20 dB), and therefore, this antenna also has linear polarization. In Ant. 3 by adding rectangular slots to the antenna, the axial ratio is reduced drastically to 8–15 dB, and in this case, we have linear polarization, but the antenna shows more tendency for achieving circular polarization. However, for achieving circular polarization in this case, we add a metamaterial load to the antenna. In the prototype antenna, we achieve circular polarization with an axial ratio less than 3 dB in the range of 2.9–3.65 GHz. Fig. 5(b) shows the measured and simulated

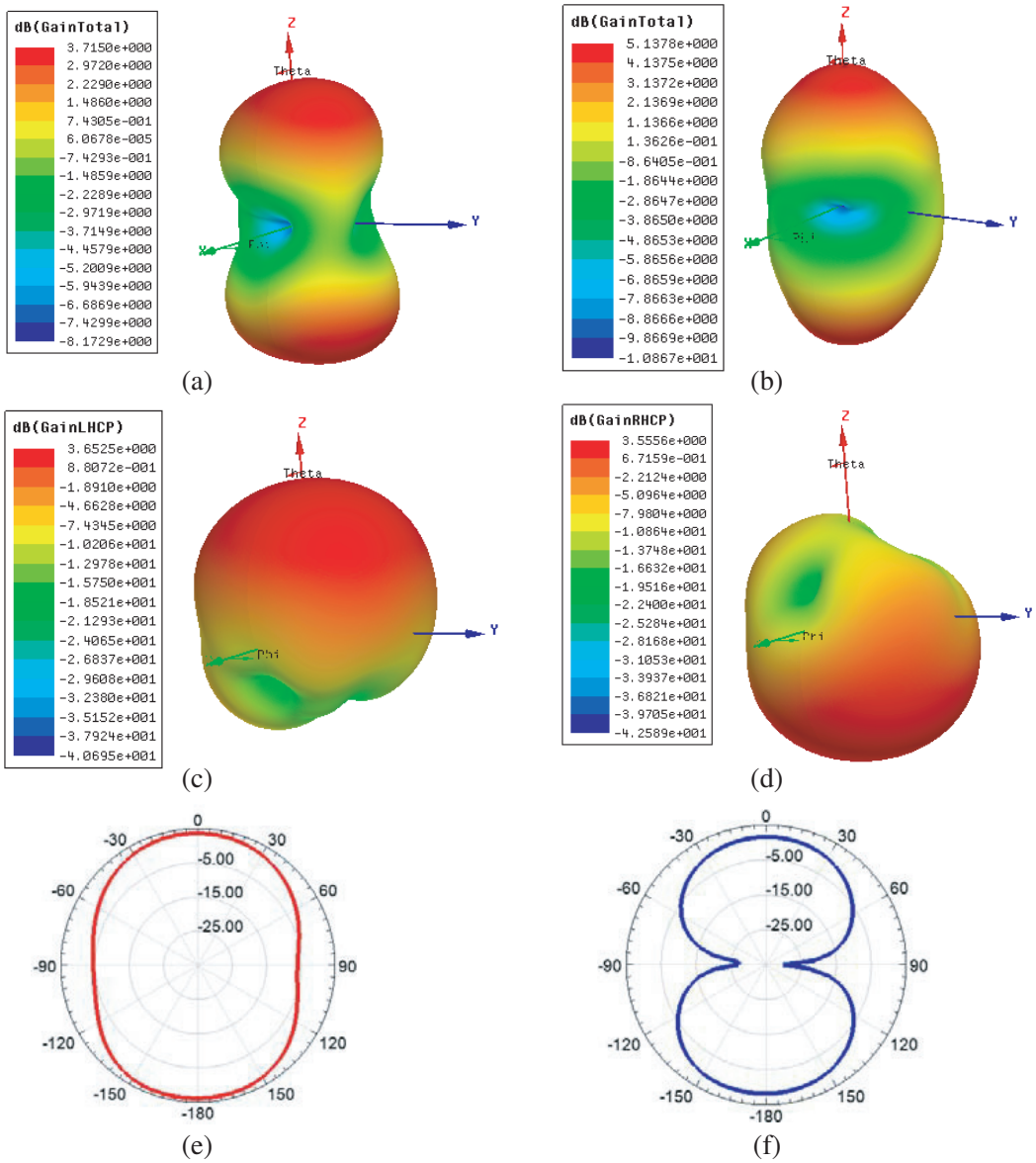

Figure 6. Radiation patterns. (a) 3D pattern at 3.4 GHz, (b) 3D pattern at 4.2 GHz, (c) pattern for LHCP at 3.4 GHz, (d) pattern for RHCP at 3.4 GHz, (e) measured E-plane pattern at 3.4 GHz, (f) measured H-plane pattern at 3.4 GHz.

axial ratios of the final antenna.

The simulated and measured radiation patterns of the antenna are presented in Fig. 6. The antenna 3D pattern simulations for 3.4 and 4.2 GHz are presented in Figs. 6(a) and 6(b). The antenna radiates omni-directionally in the E-plane and approximately bi-directionally in the H-plane.

In addition, the antenna 3D patterns for LHCP (left-hand circular polarization) and RHCP (right-hand circular polarization) at 3.4 GHz are shown, respectively, in Figs. 6(c) and 6(d). As shown here, the antenna gains are 3.71 dBi for the total gain and 3.65 and 3.55 dBi for LHCP and RHCP, respectively, at 3.4 GHz Therefore, the prototype antenna shows circular polarization. The measured radiation patterns (co-polarization) of the prototype antenna at 3.4 GHz in the E-plane (y-z plane) and H-plane (x-z plane) are shown in Figs. 6(e) and 6(f).

The antenna gain and efficiency are presented for the antenna, presented in Fig. 7. As shown here, the antenna efficiency is more than 85% for the first band and more than 80% for the second band and typically is more than 80% in the range 2–5 GHz. The antenna gain is simulated and compared to the measured value, and is around 3–4 dBi.

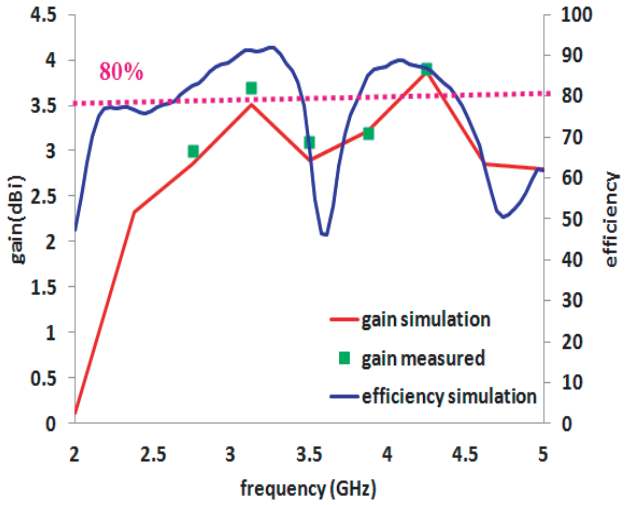

Figure 7. Simulated and measured gain, and simulation efficiency.

5. CONCLUSION

A novel shape for SRR is modified for achieving dual-bandwidth characteristics and circular polarization for Wi-Fi and WiMAX applications. The antenna magnitude of S_{11} is compared in each case to show the element effect on the antenna. The final antenna efficiency is more than 8% for 2–5 GHz. In this antenna, parasitic elements and slots are used to generate a symmetrical distribution that results in circular polarization in the antenna. We also show how the metamaterial characteristics of the unit cell affect antenna circular polarization.

In this antenna, we develope novel parasitic elements and slots to control the current distribution that results in circular polarization in the antenna. In comparison with our previous research [32, 33], in this paper, we show how the split ring produces double negative characteristics, and the antenna shows good axial ratio where we have negative characteristics.

REFERENCES

1. Al Farooqui, M. A., J. Breeland, M. I. Aslam, M. Sadatgol, ç. K. Özdemir, M. Tame, L. Yang, and D. Ö. Güney, "Quantum entanglement distillation with metamaterials," *Optics Express*, Vol. 23, No. 14, 17941–17954, 2015.

2. Zhang, X., E. Usi, S. K. Khan, M. Sadatgol, and D. O. Gueney, "Extremely sub-wavelength negative index metamaterial," *Progress In Electromagnetics Research*, Vol. 152, 95–104, 2015.
3. Sanada, A., C. Caloz, and T. Itoh, "Characteristics of the composite right/left-handed transmission lines," *IEEE Microwave and Wireless Components Letters*, Vol. 14, No. 2, 68–70, 2004.
4. Buell, K., H. Mosallaei, and K. Sarabandi, "A substrate for small patch antennas providing tunable miniaturization factors," *IEEE Transactions on Microwave Theory and Techniques*, Vol. 54, No. 1, 135–146, 2006.
5. Ziolkowski, R. W., and N. Engheta, "Metamaterial special issue introduction," *IEEE Transactions on Antennas and Propagation*, Vol. 51, No. 10, 2546–2549, 2003.
6. Smith, D. R., S. Schultz, P. Markoš, and C. M. Soukoulis, "Determination of effective permittivity and permeability of metamaterials from reflection and transmission coefficients," *Physical Review B*, Vol. 65, No. 19, 195104, 2002.
7. Marqués, R., F. Mesa, J. Martel, and F. Medina, "Comparative analysis of edge-and broadside-coupled split ring resonators for metamaterial design-theory and experiments," *IEEE Transactions on Antennas and Propagation*, Vol. 51, No. 10, 2572–2581, 2003.
8. Kim, J., C. S. Cho, and J. W. Lee, "5.2 GHz notched ultra-wideband antenna using slot-type SRR," *Electronics Letters*, Vol. 42, No. 6, 315–316, 2006.
9. Kim, C., J. Jang, Y. Jung, H. Lee, J. Kim, S. Park, and M. S. Lee, "Design of a frequency notched UWB antenna using a slot-type SRR," *AEU-International Journal of Electronics and Communications*, Vol. 63, No. 12, 1087–1093, 2009.
10. Park, W.-K., S.-T. Han, and S.-S. Oh, "Frequency-tunability of a miniaturized waveguide filter loaded with a split-ring-resonator," *Microwave and Optical Technology Letters*, Vol. 55, No. 7, 1649–1653, 2013.
11. Estep, N. A., A. N. Askarpour, and A. Alu, "Experimental demonstration of negative-index propagation in a rectangular waveguide loaded with complementary split-ring resonators," *IEEE Antennas and Wireless Propagation Letters*, Vol. 14, 119–122, 2015.
12. Yoon, K.-C., J. H. Kim, and J.-C. Lee, "Band-pass filter with broad-side coupled triple split-ring resonator using left-handed metamaterial," *Microwave and Optical Technology Letters*, Vol. 53, No. 9, 2174–2177, 2011.
13. Safwat, A. M. E., S. Tretyakov, and A. Räisänen, "Dual bandstop resonator using combined split ring resonator and defected ground structure," *Microwave and Optical Technology Letters*, Vol. 49, No. 6, 1249–1253, 2007.
14. Zhu, S., D. G. Holtby, K. L. Ford, A. Tennant, and R. J. Langley, "Compact low frequency varactor loaded tunable SRR antenna," *IEEE Transactions on Antennas and Propagation*, Vol. 61, No. 4, 2301–2304, 2013.
15. Zuffanelli, S., G. Zamora, P. Aguila, F. Paredes, F. Martin, and J. Bonache, "On the radiation properties of Split-Ring Resonators (SRRs) at the second resonance," *IEEE Transactions on Microwave Theory and Techniques*, Vol. 63, No. 7, 2133–2141, 2015.
16. Mumcu, G., A. Dey, and T. Palomo, "Frequency-agile bandpass filters using liquid metal tunable broadside coupled split ring resonators," *IEEE Microwave and Wireless Components Letters*, Vol. 23, No. 4, 187–189, 2013.
17. Patel, S. K. and C. Argyropoulos, "Enhanced bandwidth and gain of compact microstrip antennas loaded with multiple corrugated split ring resonators," *Journal of Electromagnetic Waves and Applications*, Vol. 30, No. 7, 1–17, 2016.
18. Kuhestani, H., M. Rahimi, Z. Mansouri, F. B. Zarrabi, and R. Ahmadian, "Design of compact patch antenna based on metamaterial for WiMAX applications with circular polarization," *Microwave and Optical Technology Letters*, Vol. 57, No. 2, 357–360, 2015.
19. Zarrabi, F. B., Z. Mansouri, R. Ahmadian, M. Rahimi, and H. Kuhestani, "Microstrip slot antenna applications with SRR for WiMAX/WLAN with linear and circular polarization," *Microwave and Optical Technology Letters*, Vol. 57, No. 6, 1332–1338, 2015.

20. Chen, H.-M., K.-Y. Chiu, Y.-F. Lin, and S.-A. Yeh, "Circularly polarized slot antenna design and analysis using magnetic current distribution for RFID reader applications," *Microwave and Optical Technology Letters*, Vol. 54, No. 9, 2016–2023, 2012.
21. Yohandri, J. T. S. Sumantyo, and H. Kuze, "A new triple proximity-fed circularly polarized microstrip antenna," *AEU-International Journal of Electronics and Communications*, Vol. 66, No. 5, 395–400, 2012.
22. Baharuddin, M., V. Wissan, and J. T. S. Sumantyo, "Elliptical microstrip antenna for circularly polarized synthetic aperture radar," *AEU-International Journal of Electronics and Communications*, Vol. 65, No. 1, 62–67, 2011.
23. Krishna Ram, R. V. S. and R. Kumar, "Design of ultra wideband trapezoidal shape slot antenna with circular polarization," *AEU-International Journal of Electronics and Communications*, Vol. 67, No. 12, 1038–1047, 2013.
24. Pouyanfar, N. and S. A. Rezaeieh, "Dual-polarized ultra wideband CPW-fed slot antenna with reconfigurable circular polarization characteristic for WiMax and WLAN applications," *Microwave and Optical Technology Letters*, Vol. 55, No. 9, 2023–2026, 2013.
25. Row, J.-S. and Y.-D. Lin, "Miniaturized designs of circularly polarized slot antenna," *Microwave and Optical Technology Letters*, Vol. 56, No. 7, 1522–1526, 2014.
26. Qing, X. and Z. N. Chen, "Dual-square-ring-shaped slot antenna for wideband circularly polarized radiation," *Microwave and Optical Technology Letters*, Vol. 56, No. 11, 2645–2649, 2014.
27. Wang, X.-Y. and G.-M. Yang, "Dual frequency and dual circular polarization slot antenna for BeiDou navigation satellite system applications," *Microwave and Optical Technology Letters*, Vol. 56, No. 10, 2222–2225, 2014.
28. Wei, C.-Y., J.-C. Liu, S.-S. Bor, T.-F. Hung, and C. C. Chen, "Compact single-feed circular slot antenna with asymmetrical C-shaped strips for WLAN/WiMAX triband and circular/elliptical polarizations," *Microwave and Optical Technology Letters*, Vol. 55, No. 2, 272–278, 2013.
29. Pouyanfar, N., "Broadband square slot circularly polarized antenna for WiMAX and WLAN applications," *Microwave and Optical Technology Letters*, Vol. 55, No. 9, 2191–2195, 2013.
30. Naser-Moghadasi, M., R. Ahmadian, Z. Mansouri, F. B. Zarrabi, and M. Rahimi, "Compact EBG structures for reduction of mutual coupling in patch antenna MIMO arrays," *Progress In Electromagnetics Research C*, Vol. 53, 145–154, 2014.
31. Numan, A. B. and M. S. Sharawi, "Extraction of material parameters for metamaterials using a full-wave simulator [education column]," *IEEE Antennas and Propagation Magazine*, Vol. 55, No. 5, 202–211, 2013.
32. Pirooj, A., M. Naser-Moghadasi, and F. B. Zarrabi, "Design of compact slot antenna based on split ring resonator for 2.45/5 GHz WLAN applications with circular polarization," *Microwave and Optical Technology Letters*, Vol. 58, No. 1, 12–16, 2016.
33. Rahimi, M., M. Maleki, M. Soltani, A. S. Arezomand, and F. B. Zarrabi, "Wide band SRR-inspired slot antenna with circular polarization for wireless application," *AEU-International Journal of Electronics and Communications*, 2016.